Journal of Marine Research, 54, 679–703, 1996

Deducing dynamic properties from simulated hydrographic data: Part I. Results from a non-eddy-resolving model

by Huai-Min Zhang[1,2] and Nelson G. Hogg[3]

ABSTRACT

Inverse models are widely used in oceanography. However, their reliability remains an open question, as comparison of inverse model results with real values of ocean parameters is difficult due to insufficient knowledge of the latter. The feasibility of extracting the ocean general circulation, mixing rates, as well as air-sea heat and freshwater fluxes from hydrographic data is studied by applying an inverse model to the CME (Community Modeling Effort) results where both the physics and parameter values are known.

The inverse model assumes approximate thermal wind balance and steady state conservation laws for mass, heat, and salt, assumptions satisfied by the GCM ocean although the residuals in the tracer conservation equations are comparable to the diffusion terms in the deep ocean. Effects of errors in these equations on inverse model solutions for different variables are studied in detail. A surface layer model is designed to estimate the air-sea heat and freshwater fluxes and the results are compared to their "true" values. Experiments on various parameterizations of different variables are carried out in the hope of getting some guidance in applying the inverse model to the real ocean.

The inverse model estimates for horizontal circulation are relatively robust—they are consistent with the GCM ocean circulations in most of the experiments, and effects of equation errors are more pronounced in the estimates for diffusivity and air-sea fluxes. Residuals in the equations are noisy and resemble a random distribution. In such cases, the estimates for all the parameters are very close to their true values. The conclusions of this work are different from previous works, and the discrepancies are explained.

1. Introduction

Oceanic circulation is an important mechanism for heat and other property transport in the global climate system. However, the picture of the world ocean general circulation is far from complete due to the difficulty and cost of direct current measurement and the uncertainty involved in extracting the time-mean part of the circulation from incomplete time series contaminated by energetic mesoscale eddies. Water property fields, on the other hand, are relatively stable and better defined from historical observations, and determina-

1. Massachusetts Institute of Technology and Woods Hole Oceanographic Institution Joint Program, Woods Hole, Massachusetts, 02543, U.S.A.

2. Present address: Physical Oceanography Research Division, Scripps Institution of Oceanography, University of California San Diego, La Jolla, California, 92093-0230, U.S.A.

3. Physical Oceanography Department, Woods Hole Oceanographic Institution, Woods Hole, Massachusetts, 02543, U.S.A.

tion of oceanic circulation from these fields dates back to the beginning of physical oceanography. Although direct current measurements are now made more frequently than ever before, it is likely that hydrographic data supplemented with chemical and biological tracers and satellite measurements will remain the principal source of information.

An early use of hydrographic data to deduce ocean circulation was the descriptive method (e.g., Wüst, 1935; Montgomery, 1938) wherein water property distributions were used to deduce large-scale flow patterns qualitatively, but no quantitative analyses were made. Furthermore, as property distributions are determined by both advective and diffusive processes, interpretation of property tongues is not entirely straightforward. Similar patterns resulting from different processes were found by Zhang and Hogg (1992). In the traditional quantitative analysis (the dynamic method), the vertical shears of horizontal velocities are calculated from the density field through the thermal wind relation. There is an intrinsic undetermined "barotropic" part and, although various ways of determining the so-called "level of no motion" have been proposed, there is neither theoretical nor observational justification for the existence of such a level. Small errors in this "barotropic" part may introduce large errors in calculating basin-wide property transports. "Inverse models" (hereafter IMs) attempt to address the inadequacies of the above two methods by seeking flow fields which are consistent with property distributions and the thermal wind relation, simultaneously (Wunsch, 1977, 1978; Stommel and Schott, 1977; Schott and Stommel, 1978).

Box IMs generally have fewer constraints than unknowns, an underdeterminacy which leads to a range of circulation patterns compatible with geostrophic balance and mass conservation (e.g., Wunsch and Grant, 1982). Wunsch (1984) argued that the range could be narrowed by adding information from other data sets. More complicated IMs infer mixing rates as well as ocean circulation with tracers such as oxygen and nutrients all used to constrain the solutions (Wunsch, 1984; Olbers *et al.,* 1985; Hogg, 1987; Jenkins, 1987; Schlitzer, 1987; Spitzer and Jenkins, 1989) and make studies of double diffusion possible (Zhang and Hogg, 1992; Lee and Veronis, 1993). Transient tracers have been treated using control theory (Wunsch, 1988a, b). The recent intensification of inverse modeling activity in oceanography is spurred onward by advances in computer power and the rapidly increasing quantity of data. *In-situ* observations of hydrography, tracers and nutrients, floats and drifters, current-meter moorings, altimetry, wind stress, and water mass fluxes across various straits and sills (e.g., Bryden *et al.,* 1994) from field programs and satellite measurements (e.g., the World Ocean Circulation Experiment) will greatly reduce the uncertainty of the physical state of the ocean. The more accurate data bring great opportunities for inverse modelers to study the oceanic general circulation and mixing processes and their roles in the climate system.

Although inverse methods are self-consistent in that they give not only estimates for parameters but also their uncertainties, direct comparison of IM results against reality is not possible due to the lack of direct measurements. This leaves the artificial ocean of a numerical model as the only feasible domain in which to validate an IM [e.g., the channel models of Fiadeiro and Veronis (1984) and Lee and Veronis (1989); Bigg's (1985) and

Killworth's and Bigg's (1988) work in GCM oceans]. In testing Schott's and Stommel's (1978) β-spiral method in a non-eddy-resolving GCM ocean, Bigg (1985) found that the estimated spirals differed about 0.5 cm/s from the GCM "data" although their shapes were similar (c.f. his Fig. 1). Adding diffusion to the model, the estimates for velocities and diffusivity remained significantly different from the GCM ocean values and sensitive to the number of layers and the choice of the reference depth. Intercomparison of three IMs in an eddy-resolving GCM ocean (Killworth and Bigg, 1988) were not promising although, as no uncertainties from the inversion were given, one could not judge the significance of the discrepancies.

Conclusions of Bigg (1985) and Killworth and Bigg (1988) raise doubts about the reliability of inverse models, especially those derived from the β-spiral method. The subject of "validating" or properly interpreting IM results is pursued in the present work. Oceanography has reached a stage of maturity such that estimates of parameters without corresponding estimates of uncertainty are no longer very useful. Also, as the physics of IMs are usually simpler than those of the (GCM or real) oceans in which they are tested, it is essential to analyze how accurately the IMs approximate the oceans. Furthermore, the issue of representing the GCM oceans by the IMs should be separated from representing the real ocean by the IMs, as the physics of any GCM ocean is also simpler than that of the real ocean. The beta-spiral method tested by Bigg (1985) and Killworth and Bigg (1988) did not include conservation equations for heat and salt and other tracers. Additional constraints such as these should improve the parameter solutions in terms of their statistical closeness to the "true" values and/or the solution resolution (Wunsch, 1989; Zhang and Hogg, 1992), especially when diffusivity is also estimated by the model.

The reliability of such an IM will be examined in a non-eddy-resolving GCM ocean context. In this simple case, a clear understanding of the source and structure of the equation error is available and its effect on the IM solutions for different variables is studied in detail. Biased answers result from an incorrect model, whereas a correct model must produce consistent results. A simple model is also designed to estimate the air-sea heat and freshwater fluxes which are compared to their "true" values, and experiments on the parameterization of some variables are carried out in the hope of obtaining guidance in applying the IM to the real ocean. A second paper will deal with the application of the IM in an eddy-resolving GCM ocean, a better mimic of the real ocean.

2. The models

In order to examine closely the behavior of an IM in a GCM ocean it is essential to determine how accurately the IM represents the GCM ocean. If the two have the same physics or the discrepancies are statistically negligible, the IM estimates should be statistically consistent with the GCM ocean values. In the presence of discrepancies the ability of inverse techniques to make useful parameter estimates for velocities, mixing rates, and air-sea heat and freshwater fluxes from hydrographic data is the main theme of this study. We first describe the physics of the GCM and the IM.

The numerical GCM is the 3-D primitive equation model of the ocean developed at the

Geophysical Fluid Dynamics Laboratory (Bryan, 1969; Cox, 1984). The momentum equations are the unsteady, nonlinear Navier-Stokes equations with the Boussinesq approximation, the hydrostatic assumption, and a turbulent viscosity parameterization of the stresses exerted by subgrid scale motions. Water property (potential temperature, salinity, etc.) evaluation is obtained by integrating the nonsteady conservation equations forward in time, again utilizing a turbulent mixing hypothesis to represent the subgrid cell processes. The equation of state is approximated as a third-order polynomial in temperature and salinity (Bryan and Cox, 1972). Assumptions of "rigid-lid" at the ocean surface, no normal flow, and no normal property fluxes at solid boundaries are adopted. The finite difference formulation corresponds to the "B-grid" configuration of Arakawa and Lamb (1977) with central difference in space. Horizontally, T (Tracers) and u, v are staggered, with T situated in the cell centers and u, v placed at the corners. Vertically, T, u, v are located halfway through the vertical dimension of the cells, while w is located at the cell interfaces. Further information can be found in the works of Cox (1984) or Zhang (1994).

The IM being examined here was first used by Hogg (1987) in a potential density coordinate frame. However, in the present work, the GCM ocean is constructed in the geopotential z-coordinate and, as the vertical resolution (10 levels) is not small enough for interpolating the data onto potential density surfaces, the IM is reformulated for the z-coordinate. The basic assumptions are approximate geostrophic and hydrostatic balance, mass conservation (the continuity equation), and steady state conservation laws for tracers (potential temperature, salinity, etc.). The mathematical representations are

$$\psi_k - \psi_{k+1} \approx dh_{k\to k+1} = \frac{g}{\rho_0}\int_k^{k+1} \sigma dz \qquad k = 1, \ldots, N \tag{2.1}$$

$$fu = -\frac{\partial \psi}{\partial y}, \; fv = \frac{\partial \psi}{\partial x} \tag{2.2}$$

$$\frac{\partial u}{\partial x} + \frac{\partial v}{\partial y} + \frac{\partial w}{\partial z} \approx 0 \tag{2.3}$$

$$\frac{\partial (uT)}{\partial x} + \frac{\partial (vT)}{\partial y} + \frac{\partial (wT)}{\partial z} - \nabla(A\nabla T) - \frac{\partial}{\partial z}\left(K\frac{\partial T}{\partial z}\right) \approx 0 \tag{2.4}$$

where ∇ is the horizontal gradient operator, and approximate signs are used in the equations instead of equal signs to indicate explicitly the imperfection of the model.

Knowledge of air-sea heat and freshwater fluxes over the world oceans is poor and another objective of this work is to examine whether they can be estimated reliably. Assuming the wind-driven and geostrophic (u_g, v_g) circulations are the major components of flow in the surface layer, mass conservation can be written as

$$\Delta z_1 \left(\frac{\partial u_g}{\partial x} + \frac{\partial v_g}{\partial y}\right) + \nabla \cdot \mathbf{M}_E + (w_1 - w_2) = 0, \tag{2.5}$$

and the tracer conservation equation as

$$\nabla(\mathbf{u}_g T) + \frac{\nabla(\mathbf{M}_E T)}{\Delta z_1} + \frac{\partial(wT)}{\partial z} - \nabla(A\nabla T) - \frac{F_{\text{surf}} - K(T_1 - T_2)/(zT_1 - zT_2)}{\Delta z_1} = 0, \quad (2.6)$$

where Δz_1 is the surface layer thickness, F_{surf} the air-sea tracer (heat and freshwater) fluxes. $\mathbf{M}_E = \boldsymbol{\tau} \times \hat{\mathbf{k}}/\rho f$ is the Ekman transport (e.g., Pedlosky, 1987), and $\boldsymbol{\tau}$ the wind stress. The quantities w_1, w_2 are the vertical velocities at the sea surface and at the bottom of the surface layer, while T_1, T_2 are the tracer values at the middle depths (zT_1 and zT_2) of the surface layer and the layer immediately beneath it.

The input (knowns) for the IM are tracer (potential temperature, salinity) concentrations, density $\rho = \rho(S, T, p)$ from the equation of state, dynamic height (dh) from Eq. (2.1), and wind stress. The unknowns to be estimated are the streamfunction ψ, vertical velocity w, turbulent diffusion coefficients A and K, and air-sea heat and freshwater fluxes. Equations are finite-differenced as in the GCM. Instead of solving for a reference velocity as is done in most traditional IMs, the absolute velocities together with other parameters are simultaneously solved for on all the model depths. The thermal wind relation is used as are mass, heat, and salt conservation constraints, and residuals are allowed in all of them. As the circulation in the deep ocean is weaker than that in the upper ocean, the relaxation of the dynamic constraint has most impact on deep circulation patterns.

Experience in applying this IM in the oceans (Hogg, 1987; Zhang and Hogg, 1992; Zhang, 1994) shows that it usually results in an overdetermined system of full rank. Solutions are obtained by minimizing the equation residual norm in the least squares sense, and no constraints on the parameter (solution) norm are used. In an underdetermined system, or an apparently overdetermined system with deficient rank, solution (parameter) norm, or a combination of solution norm and equation residual norm, is minimized, making solutions sensitive to *a priori* information such as the choice of a reference level. Even in an overdetermined system there remain subjective issues such as the row scaling.

3. Application of the IM in a non-eddy-resolving GCM ocean

In this section we examine the behavior of the IM in a non-eddy-resolving GCM provided by Spall (1992) which was configured with a grid resolution of 2° in latitude and longitude and a maximum of 10 levels in the vertical in the North Atlantic Basin extending from the equator to 64N and from 80W to 10W with "real" topography (Fig. 1). The turbulent coefficients of horizontal dissipation are 4×10^8 cm^2/s (viscosity) and 1×10^7 cm^2/s (diffusion), and the coefficients of vertical viscosity and diffusion are 1 cm^2/s. Heat flux at the sea surface was parameterized by relaxation of the temperature at the uppermost level in the model to the apparent atmospheric temperature (Han, 1984), and surface freshwater flux by a similar relaxation of the salinity to the climatological mean surface salinity of Levitus (1982). Surface wind forcing was taken from the annual mean winds derived by Hellerman and Rosenstein (1983). Boundary conditions, initialization of

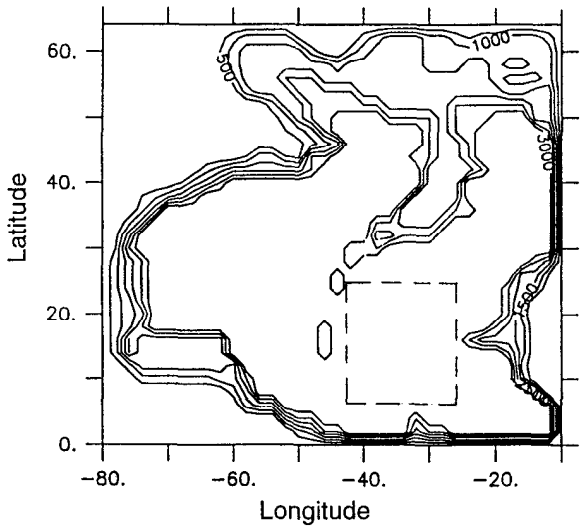

Figure 1. Topography of the numerical GCM ocean (Spall, personal communication). The dashed line box is the inverse model domain.

the model and other information can be found in Spall (1992). The numerical ocean state used in this work is chosen as the final, instantaneous state after 400 years of integration.

a. Accuracy of the IM in the GCM ocean

The inverse model is tested in a subdomain of the GCM ocean. This subdomain, which extends from 42W to 26W and 7N to 25N (Fig. 1), is so chosen that the assumptions of the IM tend to hold and the topographic effects are minor as the bottom is flat at 4000 m. To have a better understanding of the IM behavior in the GCM ocean we first examine the IM accuracy in this subdomain.

Dynamic equation: The IM dynamic equation is the approximate thermal wind relation. Thermal wind shears can be computed from the GCM density field and directly compared to the shears of the absolute horizontal velocities (Fig. 2). Shown in Figure 2 are examples for the zonal velocity in the IM domain. The GCM ocean circulations are approximately in thermal wind balance except in the surface layer (Fig. 3). To quantify the imbalances, area-averaged ratios are computed as

$$R_u^2 = \frac{\Sigma(u_r - u_r dyn)^2}{\Sigma u_r^2} \tag{3.1}$$

$$R_v^2 = \frac{\Sigma(v_r - v_r dyn)^2}{\Sigma v_r^2} \tag{3.2}$$

where u_r, v_r are the actual velocity shears, $u_r$dyn, $v_r$dyn the thermal wind shears, and the summation is taken over the horizontal IM domain. Although visually (Fig. 2) the GCM

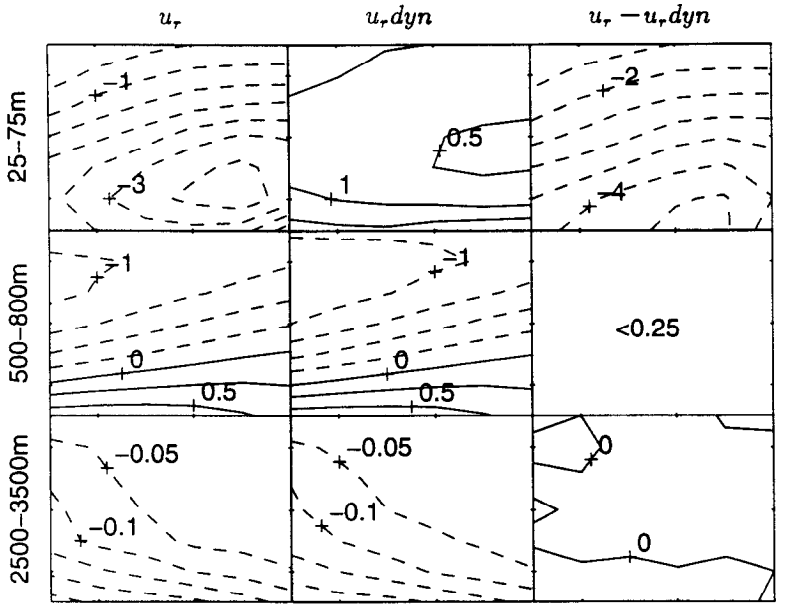

Figure 2. Lateral distributions, within the IM domain, of the difference in zonal velocity computed between the two depths indicated to the left of each row. The first column (u_r) gives the actual velocity difference, the second ($u_r dyn$) is that derived from the thermal wind relation, and the third is the difference between the first two. Units are cm/s.

ocean circulations are in good thermal wind balance, the area-averaged imbalances have vertical mean values of 16% and 12.5% in the zonal and meridional directions below the surface layer (Table 1).

Surface layer model: In the surface layer IM, it is assumed that the wind-driven and geostrophic components comprise the major part of the horizontal circulation. Computing the wind-driven velocities (u_e and v_e) by dividing the Ekman transport by a surface layer depth of 50 m, the assumption is approximately satisfied (Fig. 3): the area-averaged imbalance ratios are 5.0% and 6.6% for u and v respectively.

Conservation equations for water properties: As w is diagnostically computed from the continuity equation in the GCM ocean, mass conservation is exact. Terms in the GCM heat conservation equation are shown in Figure 4 at three depths; the salt balance is similar. The advection terms are calculated, as in the IM, for the concentration anomaly $T' = T - \overline{T}$ instead of the concentration T itself, in order to reduce errors associated with these dominant terms (Hogg, 1987; Zhang, 1994). $\overline{T}$ is the horizontal mean at the depth concerned. Replacing T by T' only affects the magnitudes of the individual advection terms $\nabla \cdot (\mathbf{u}T)$ and $(wT)_z$, but not their sum $\nabla \cdot (\mathbf{u}T) + (wT)_z$, or the diffusion terms, as the continuity equation is exact in this case. Although the GCM ocean is non-eddy-resolving and forced by steady wind stress and air-sea fluxes, the oceanic state after 400 years of integration remains time dependent (Fig. 4) especially in the deep layers where the time

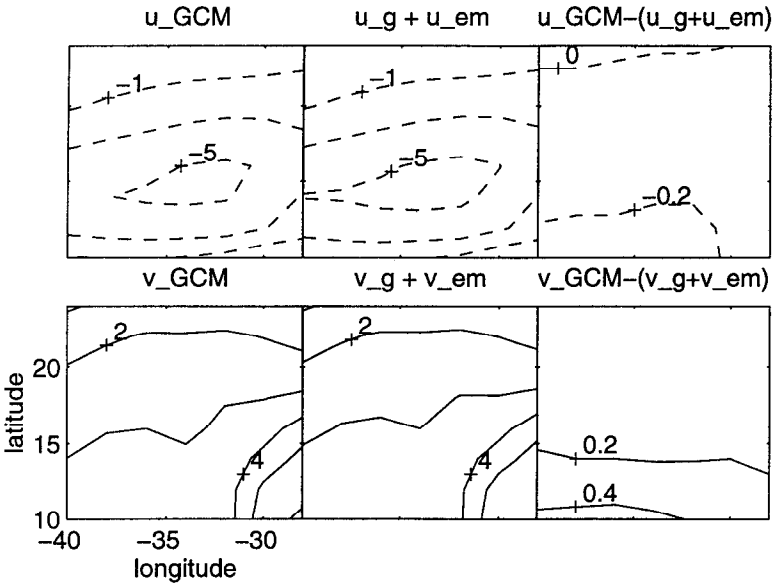

Figure 3. Horizontal velocities (cm/s) at 25 m depth in the IM domain: the first column gives GCM ocean absolute velocities; the second is the sum of geostrophic and wind-driven velocities; and the third their difference. The top row is for the zonal velocity component and the bottom for the meridional.

variation terms are large compared to the diffusion terms, and serve as model errors in the steady IM. Horizontal distributions of these terms are much more irregular than those for advection and diffusion but are similar on all the 10 vertical levels and similar to those for vertical advection at great depth. On levels 7 to 9 (at depths of 1250, 1750 and 2500 m), the major balances (for T') are between vertical advection and time variation. Therefore, neglecting the time variations in the IM should most affect the solutions for w in the deep ocean.

b. Inverse model results

In a sequence of experiments the IM is first applied to the part of the water column where it has high accuracy. Then the surface layer is incorporated into the model to estimate the air-sea heat and freshwater fluxes. Thirdly, the IM is applied in a water column where the

Table 1. Imbalance ratios between the thermal wind shear and actual velocity shear in the GCM ocean.

Depth intervals (m)	25 – 75	75 – 150	150 – 300	300 – 500	500 – 800	800 – 1250	1250 – 1750	1750 – 2500	2500 – 3500
R_u	1.40	0.14	0.29	0.24	0.13	0.07	0.23	0.09	0.09
R_v	1.06	0.14	0.16	0.14	0.08	0.07	0.16	0.12	0.13

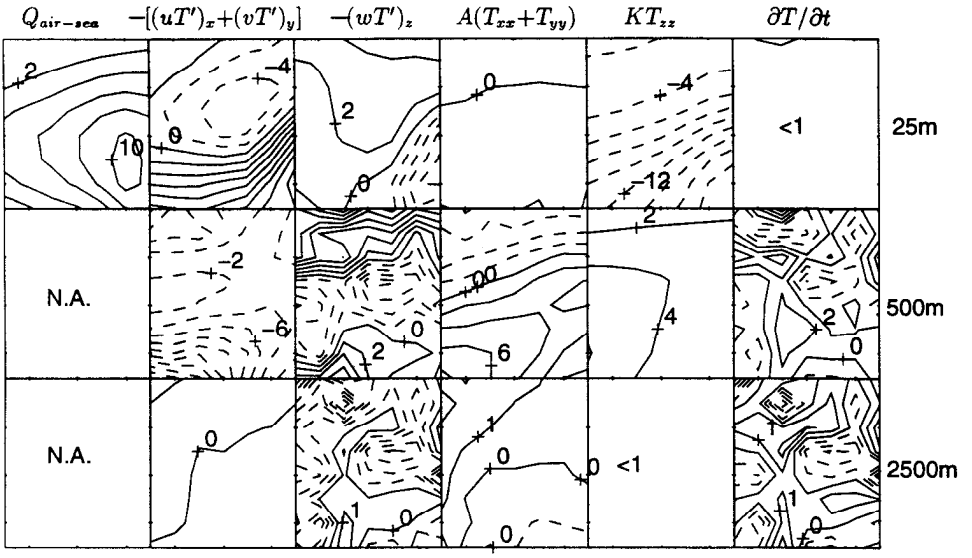

Figure 4. Terms in the heat conservation equations of the GCM ocean in the IM cells centered at 25, 500, and 2500 m depths. Solid lines are positive and dashed lines negative. Units are 10^{-8}, 10^{-9} and 10^{-10} K/s at the three depths.

model errors are larger to see how they affect IM solutions. After that, using the known "errors" in the conservation equations, experiments are carried out to see whether the parameter values can be fully recovered. Finally, experiments are carried out on the parameterization of different variables.

Although the parameter values to be estimated are known in the GCM ocean they are not used to constrain the IM solutions; instead, they are used for validation purposes. The GCM ocean circulation is shown in Figure 5: velocities are stronger on the upper levels than on the deeper ones. Figure 6 shows the vertical velocity at three depths (the upper panel) and a spatially smoothed version of it (the lower panel). The horizontal and vertical diffusion coefficients are $A = 1.00 \times 10^7$ cm^2/s and $K = 1.00$ cm^2/s, respectively. The IM grid resolution is the same as in the GCM ocean.

i. Upper layer model results. Geostrophic balance does not hold in the surface layer, and the model errors in the IM tracer conservation equations are larger than the diffusion terms at the deep levels (Fig. 4); thus we first run the IM in a water column including only the levels at 75, 150, 300, 500, 800, and 1250 m. Vertical velocities are estimated at 7 interfaces from 50 to 1500 m. To be consistent with the GCM ocean, the unknown diffusion coefficients A and K are taken as constant, while the velocity parameters (the streamfunction and vertical velocity) are pointwise unknowns. In theory equations should be scaled by the error covariance matrix (Wunsch, 1989) of the equation residuals. In practice and for simplicity, the IM tracer conservation equations are scaled by the horizontally-averaged

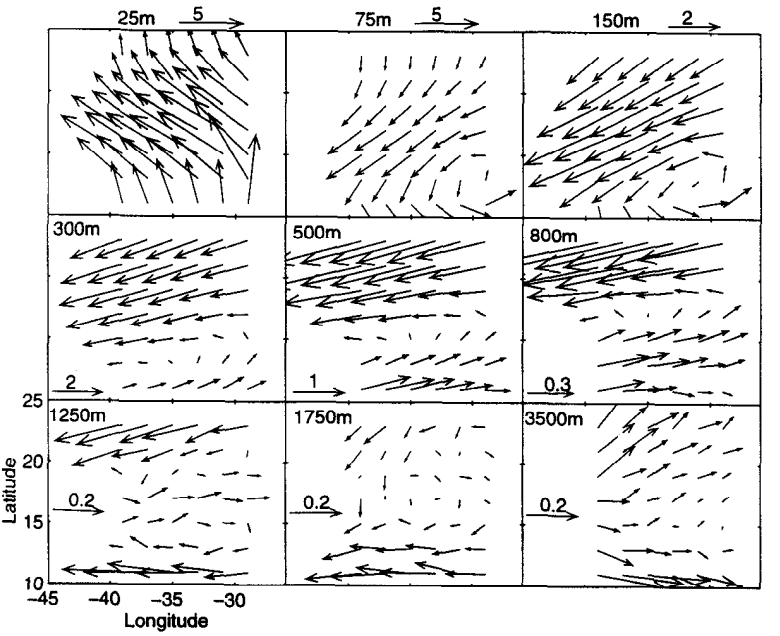

Figure 5. The GCM ocean circulation at 9 depths. Note the changing velocity scale (in cm/s).

norm of the model errors. In the real ocean, complete statistics of model equation errors are usually unknown. Equation scaling without this information was discussed by Zhang and Hogg (1992) (examples are also seen in the present and the follow-up paper) where the relative weighting factors among different equations (the dynamic equation, the conserva-

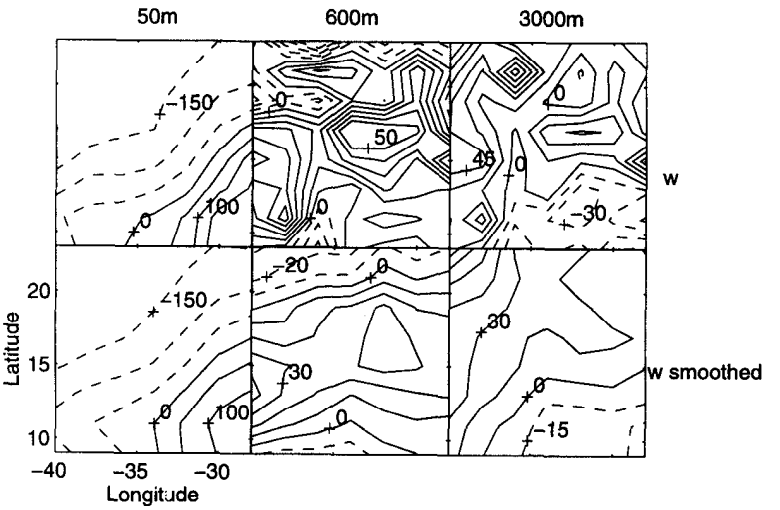

Figure 6. The GCM ocean vertical velocities (10^{-6} cm/s) at 3 depths (the upper panel) and a 9-point horizontally smoothed version (the lower panel).

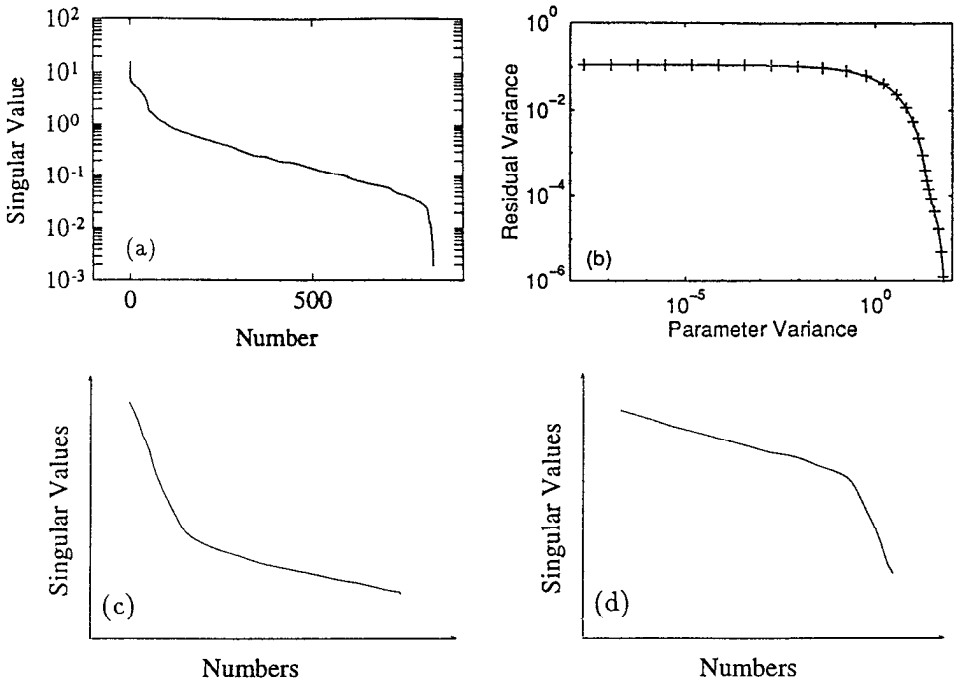

Figure 7. (a) Singular value profile of the equation system; (b) Levenberg-Marquardt stabilization diagram; (c) same as in (a) but the dynamic equation is downweighted; and (d) same as in (a) but the dynamic equation is highly weighted. Profiles in (c) and (d) are schematic.

tion equations for mass, heat, and salt) were chosen experimentally so that the scaled residuals are of the same magnitude. Contributions of individual equations to the solution can be identified by the data resolution matrix (Wunsch, 1989).

The finite difference of the IM equations results in an equation system of 820 unknowns in 1363 equations. Analyses of the singular values (Fig. 7a) and the Levenberg-Marquardt stabilization diagram (Fig. 7b, see Lawson and Hanson, 1974) show that the equation system is overdetermined and of full rank.

A first glance at the singular value profile (Fig. 7a) might lead one to think that the system is singular because of the rapid drop in singular value at large number. A detailed analysis shows that this is not the case. In fact, due to the scaling of the equations, the singular values associated with the dynamic equations (the flatter segment in Fig. 7a) are in the (middle) range of the eigenvalues associated with the conservation equations for mass, heat and salt (the two segments with large slopes at the beginning and the end of the profile). When the dynamic equations were further downweighted, their associated singular values (the flatter segment) migrated downward, and the two large-slope segments associated with the conservation equations were linked together at the beginning (Fig. 7c). On the other hand, when the dynamic equations were highly weighted, their associated singular values migrated upward, and the two large-slope segments connected each other again but at the end (Fig. 7d). Truncating the rapidly dropping singular values in Figure 7d

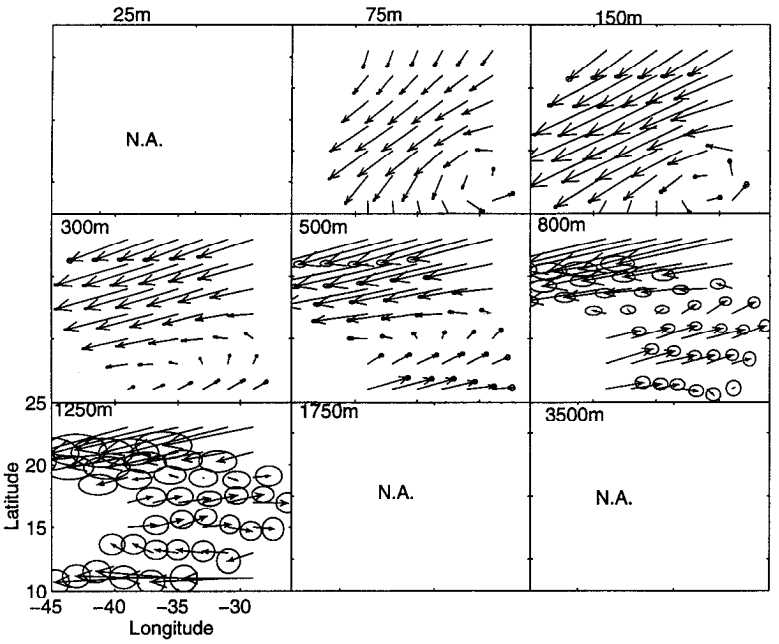

Figure 8. The Upper Layer Model estimates for horizontal circulation with their 95% confidence error ellipses. Velocity scales are the same as in Figure 5.

and their associated eigenvectors to obtain the solutions would remove the contributions from the conservation equations. This can be confirmed by the data resolution matrix (Wunsch, 1989): elements corresponding to the dynamic equations are nearly unity while those of the conservation equations are nearly zero. In such a case the absolute velocities and the diffusion parameters (which only appear in the conservation equations) will not be determined accurately. Although an abrupt drop in singular values can indicate singularity, a detailed analysis and other tools, such as the Levenberg-Marquardt stabilization analysis (Fig. 7b) can indicate otherwise (Hogg, 1987). Further discussion has been presented by Zhang (1994).

The IM estimated diffusion coefficients are $A = (1.08 \pm .02) \times 10^7$ cm^2/s and $K = (1.03 \pm .01)$ cm^2/s. Errors are estimated as by Zhang and Hogg (1992) and quoted herein for the 95% confidence interval. Although the estimates are very close to their "true" values of 1×10^7 cm^2/s and 1 cm^2/s, the offsets are significant. These discrepancies are attributable to the differences in the physics of the IM and the GCM ocean. As shown before the time variation terms, neglected in the IM tracer conservation equations, have the same or even larger magnitudes than the diffusion terms at depth. Although treated as noise, the time variation terms are not purely "white" and systematic offsets could cause systematic biases in parameter values.

The IM estimated circulation (Fig. 8) has the same pattern as the GCM ocean (Fig. 5) on all six levels. Velocities are also consistent within their errors at most of the grid points on

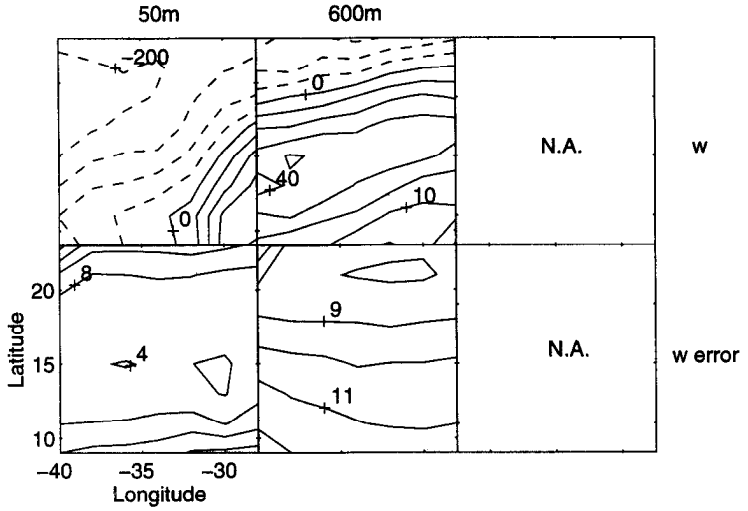

Figure 9. The Upper Layer Model estimates for vertical velocity (10^{-6} cm/s) at two depths (upper panel) and their errors (the lower panel).

all but the deepest level where the circulations are very weak. In addition to the different physics in the tracer conservation equations mentioned above, the small yet significant discrepancies in circulation can be attributed, as well, to the differences in the momentum equations of the IM and the GCM ocean. The GCM circulation deviates from the thermal wind relation by 16% in zonal and 12.5% in meridional on average (Table 1) and a close inspection of Figures 8 and 5 shows that the discrepancies are mainly in the zonal direction. The estimated meridional velocities are generally consistent even though they are weaker than the zonal velocities, especially at depth.

The estimated vertical velocity component is shown in Figure 9 at three depths together with its estimated errors. On the top four levels at 50, 100, 200 and 400 m, the estimates have the same pattern as those in the GCM ocean (Fig. 6) and the values are statistically consistent. At depths of 600, 1000 and 1500 m, differences become apparent although they are generally not significant because of the large uncertainties in the estimates. The GCM ocean vertical velocities are highly variable in space while those from the inversion are much smoother. In fact, the latter are much closer to the spatially smoothed GCM ocean w fields (Fig. 6).

ii. Determining the air-sea surface fluxes. Our present knowledge of the global air-sea heat and freshwater fluxes is poor (e.g., the most used freshwater budget in the global oceans is still the work by Baumgartner and Reichel, 1975). In this section, we incorporate the surface layer model into the IM to see how well these parameters can be estimated. Furthermore, the GCM ocean has more complicated physics in the surface layer and more assumptions or approximations are used in the IM, and these introduce larger uncertainties.

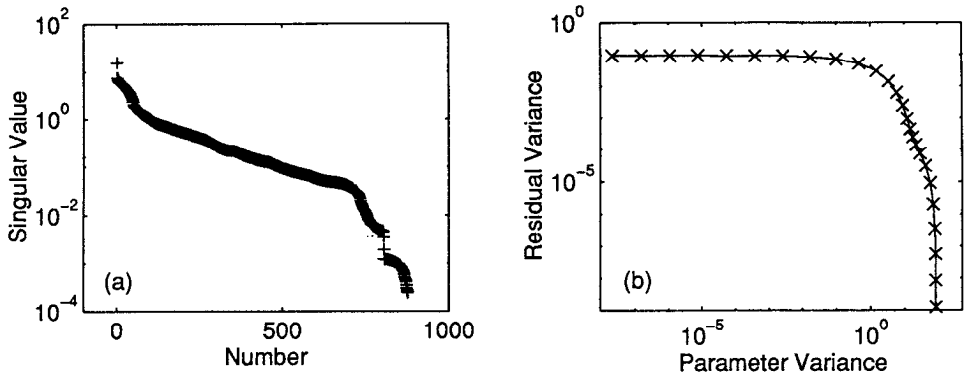

Figure 10. (a) Singular value profile, and (b) Levenberg-Marquardt stabilization diagram of the experiment involving determination of the air-sea fluxes.

Accordingly small weights (a factor of 0.01) are given to the equations in the surface layer; thus the "barotropic" part of the circulation and the diffusive parameter values are mainly determined by the constraints in the layers below and used in the surface layer heat and salt conservation equations to determine the air-sea heat and freshwater fluxes. With this configuration, the singular values of the equation system are shown in Figure 10a. Detailed analysis shows that the singular value drop at the tail does not indicate singularity of the system; instead they are the contributions from the surface layer equations, and the jump is caused by the small weight given to these equations. The nonsingularity is confirmed by the Levenberg-Marquardt stabilization diagram (Fig. 10b): small singular values contribute significantly to the reduction in residual variance without inordinate increases in parameter variance (Lawson and Hanson, 1974).

As the surface layer equations are downweighted, the IM estimates for the parameters in the layers beneath are similar to those in the previous section with larger errors: $A = (1.08 \pm 0.04) \times 10^7$ cm^2/s and $K = (1.03 \pm .02)$ cm^2/s and similarly for the velocity components. In the surface layer the geostrophic component of the horizontal circulation is estimated by the IM. The total horizontal velocity at 25 m can be calculated as $\mathbf{u}_g + \mathbf{M}_e/\delta_e$ (Fig. 11), where $\mathbf{M}_e$ is the Ekman transport and δ_e the Ekman layer depth taken as 50 m in this case. The estimated circulation at 25 m is consistent with the GCM (Fig. 5). The IM estimated air-sea heat and freshwater fluxes are shown in Figure 12 together with those values in the GCM ocean: again patterns are similar and the values are statistically consistent. Estimates in the surface layer have larger solution errors as the IM equations have larger uncertainties.

iii. Deep layer model results. As mentioned before, the error in the IM conservation equations is quite large in the deep water and results from the neglected time variation terms. In this section we examine the effect of this error on the IM solutions. Six deeper levels are chosen with the cells centered at the depths of 300, 500, 800, 1250, 1750 and

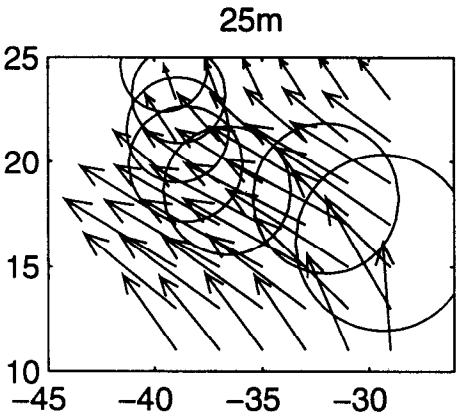

Figure 11. IM estimated absolute horizontal velocities in the surface layer (at 25 m). Error ellipses are subsampled for easier reading and they depend mostly on latitude. The velocity scale is the same as in Figure 5.

2500 m. Model error is smaller than the other terms in the IM conservation equations only in the two uppermost layers.

The IM estimates for the horizontal circulation are once again generally statistically consistent with the GCM ocean ones. The estimated vertical velocity fields are similar to the horizontally smoothed vertical velocity fields of the GCM ocean, and the values are generally consistent within the estimated error bars. However, the IM estimated diffusion coefficients are $A = (0.98 \pm 0.01) \times 10^7$ cm^2/s and $K = 0.86 \pm 0.02$ cm^2/s, which are further away from the GCM ocean values. In obtaining the IM solutions, minimization of the equation residuals forces the time variation terms into the physical terms of the IM (the

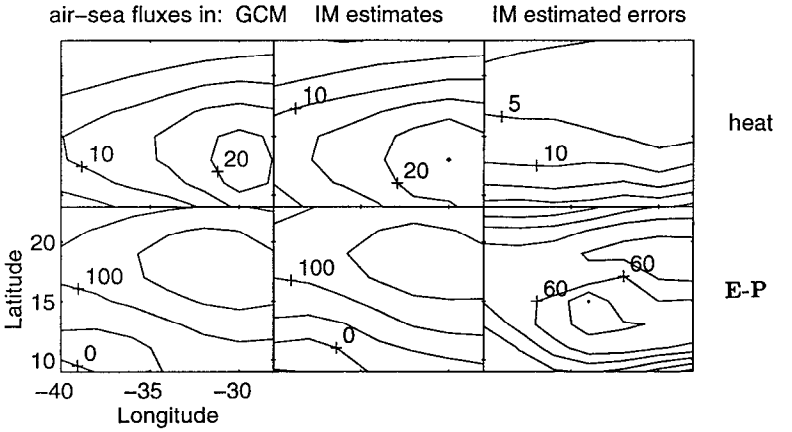

Figure 12. Air-sea heat (upper panel, W/m^2) and freshwater (lower panel, cm/yr) fluxes in the GCM ocean (the 1st column) and estimated by the IM (the 2nd column) with their expected errors (the 3rd column).

advection and diffusion terms). The parameters that are most easily adjusted are the diffusion ones as they appear only in the heat and salt conservation equations, while the parameters for velocities are further constrained by the dynamic and continuity equations. In the upper layers, where advection terms dominate diffusion ones, equation residuals are more sensitive to the change of velocities than to the change of diffusion coefficients.

To investigate further the effects of model errors on the IM solutions, the horizontal diffusion coefficient A is allowed to be a different constant on each of the 6 vertical levels. Although the number of unknowns is increased, the singular value and the Levenberg-Marquardt stabilization analyses show that the equation system remains overdetermined and of full rank and the solutions for the velocity components do not differ significantly from the previous case. The estimated diffusion coefficients are $K = 0.82 \pm 0.02$ cm^2/s and $A = (1.03 \pm 0.03, 1.01 \pm 0.03, 0.92 \pm 0.03, 0.94 \pm 0.04, 0.84 \pm 0.04, 0.64 \pm 0.04) \times 10^7$ cm^2/s on the six levels, respectively. On levels 1 and 2, where model error is small, the estimates for A are statistically consistent with the GCM value while on the deeper levels deviations become increasingly significant.

iv. Full layer model results—the standard run. We now use the IM in the whole water column from the ocean surface to the bottom (4000 m) with a total of 10 vertical layers (we label it *the standard run*). The finite differencing of the IM equations results in 2319 equations for 1328 unknowns. Analysis of the singular values, aided by the Levenberg-Marquardt stabilization diagram, shows that this equation system is also overdetermined and of full rank. Solutions are obtained by minimizing the equation residual norm with no restrictions on the size of solution (parameter) norm, yet the IM estimates all have expected magnitudes, another indication of the nonsingularity of the equation system.

Comparison of the estimated circulations (Fig. 13) with the GCM (Fig. 5) reveals statistically consistent estimates at the depths of 25, 300, 500, 800 and 1250 m. As the estimated errors are very small (except in the surface layer at 25 m), consistency indicates that the estimates are almost identical to their "true" values. At all the other depths (75, 150, 1750, 2500, and 3000 m) the differences are small yet significant. Estimates for w (Fig. 14) are also found to be similar to the GCM ocean vertical velocities (Fig. 6) both in pattern and value. However, moving down the water column, the estimates become increasingly different from the GCM vertical velocities in their detailed horizontal structures, and more similar to the horizontally smoothed version of the GCM data (Fig. 6). The estimated air-sea heat and freshwater fluxes are about the same as in the previous section and statistically consistent with the GCM ocean values. Estimates for diffusion coefficients, $A = (1.09 \pm 0.02) \times 10^7$ cm^2/s and $K = 1.03 \pm 0.02$ cm^2/s, are better than those in the deep layer model results but worse than those in the upper layer model results.

In obtaining the solutions and the solution errors the assumption of white noise (i.e. uncorrelated with zero mean) has been used. We can check the consistency of our results with this *a priori* assumption. The scaled post-solution equation residuals are more or less randomly distributed with zero mean (Fig. 15). Our estimates of parameter errors are based

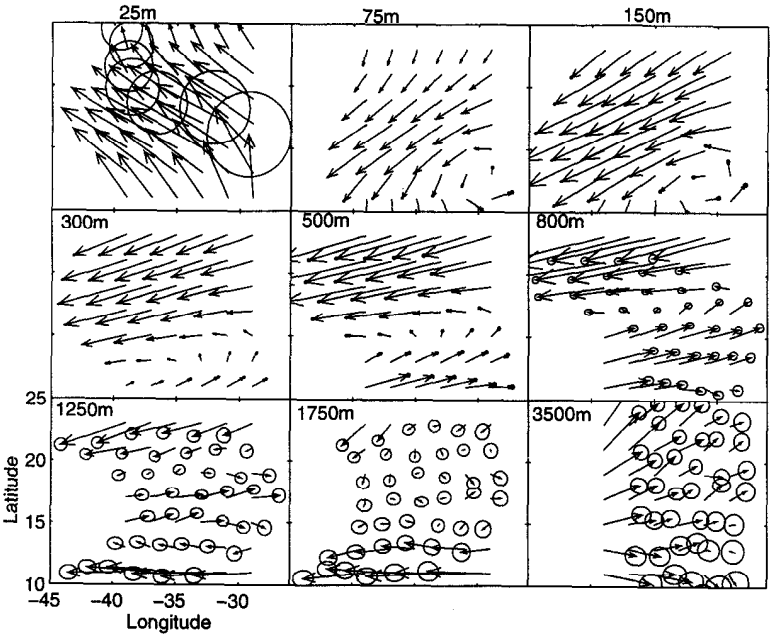

Figure 13. Estimated horizontal circulations from the standard run and their expected error ellipses, which are subsampled at 25 m for ease of reading (c.f. Fig. 11). Velocity scales are the same as in Figure 5.

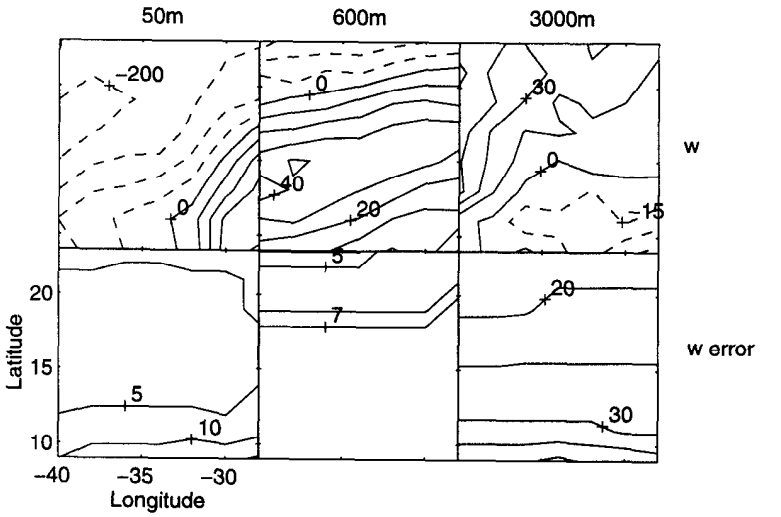

Figure 14. Estimated vertical velocities from the standard run at three depths (the upper panel) and their expected errors (the lower panel). Units are 10^{-6} cm/s.

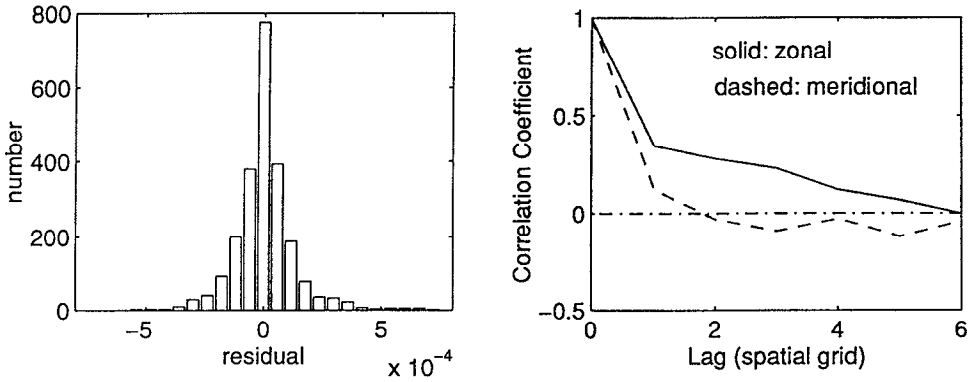

Figure 15. The distribution of the post-solution equation residuals of the standard run (left), and the spatial auto-correlations of the salt balance residuals in the zonal (right, solid line) and meridional (right, dashed line) directions.

on the assumption that all the constraints are independent (i.e. that the error covariance matrix is diagonal). Also shown in Figure 15 is the spatially lagged correlation function for the residuals from the salt balance, averaged over all the depths, but separated into zonal and meridional lags. Very similar forms are obtained for the other balances. In the meridional direction the correlation function is approximately zero at one grid spacing, supporting the notion of independence. This does not appear to be true in the zonal direction where the correlation is reduced to about 0.3 at one grid spacing and falls more slowly after that. It is clear that our numbers of degrees of freedom are not nearly as large as has been assumed in calculating the parameter errors which, consequently, should be viewed as underestimates.

The standard run and other experiments in previous sections show that in spite of the large equation errors in the deep ocean, the IM estimates for the horizontal circulation, vertical velocity, and diffusion coefficients are very close to their values in the GCM ocean for the large-scale structure. However, there exist significant differences for some parameters at certain locations due to the different physics of the IM and GCM ocean. In our special case, the model errors are known for the IM tracer conservation equations, and we can attempt to make consistent estimates by using the above information as well. In the following experiment the temporal variations are treated as known inhomogeneous terms on the right-hand side of the IM conservation equations. The equation scaling factors in this case are now chosen as by Zhang and Hogg (1992), namely the horizontally averaged tracer anomalies which effectively increase the model errors for the deeper levels. Also, the IM conservation equations are now exact and a higher weight is given to them.

The estimated diffusion coefficients, $A = (1.03 \pm 0.05) \times 10^7$ cm^2/s and $K = 0.99 \pm 0.02$ cm^2/s, are now statistically consistent with their GCM values, and the same is true for the horizontal circulation. The most interesting feature is that the small-scale structures of the estimated vertical velocity (Fig. 16) are very similar to those of the GCM ocean and

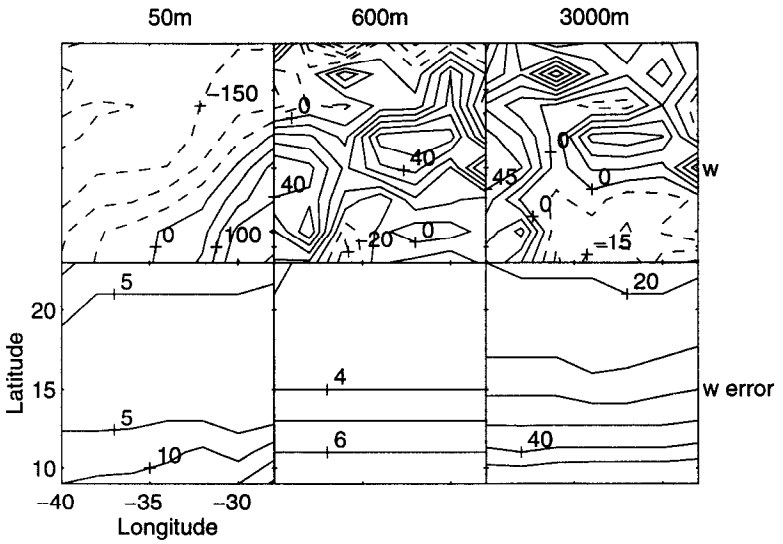

Figure 16. IM estimated vertical velocities at three depths (the upper panel) and their expected errors (the lower panel) when the time variations in the GCM tracer conservation equations were taken as known imhomogeneous terms for the IM. Units are 10^{-6} cm/s.

numerically consistent within the estimated errors. This improvement is explained by the previously mentioned fact that the temporal variation terms in the heat and salt conservation equations in the GCM ocean have the same structures as those of the vertical advection terms on the deep levels (Fig. 4): neglecting them has the most impact on w.

v. Experiments with parameterizations. In all but one of the previous experiments the diffusion coefficients A and K were treated as two unknowns, constant throughout the whole IM domain (the only exception being the deep layer model where A varied with depth). This treatment was adopted to keep the IM scheme as close to that of the GCM ocean as possible. In the real ocean, diffusion coefficients, parameterizing subgrid/mesoscale processes, are generally functions of the turbulent kinetic energy; thus functions of space and possibly also anisotropic (e.g., Figueroa and Olson, 1989; Spall *et al.*, 1993).

A straightforward approach to computing these spatially varying diffusion coefficients by the IM is to allow them to have as many degrees of freedom as possible. We could treat them as pointwise unknowns differing in the zonal and meridional directions. These formulations would result in an equation system with more unknowns than equations, thus underdetermined. For such a system, solutions are usually sought by minimizing the solution (parameter) norm. In IMs formulated for reference velocities, the kinetic energy is usually minimized and results may be sensitive to the choice of reference level. In our IM, the horizontal and vertical velocities on all the levels, diffusion coefficients, and air-sea fluxes are all unknowns and, if the system is underdetermined, what should be minimized is the norm of the deviations of the estimates from their true values, usually unknown in the

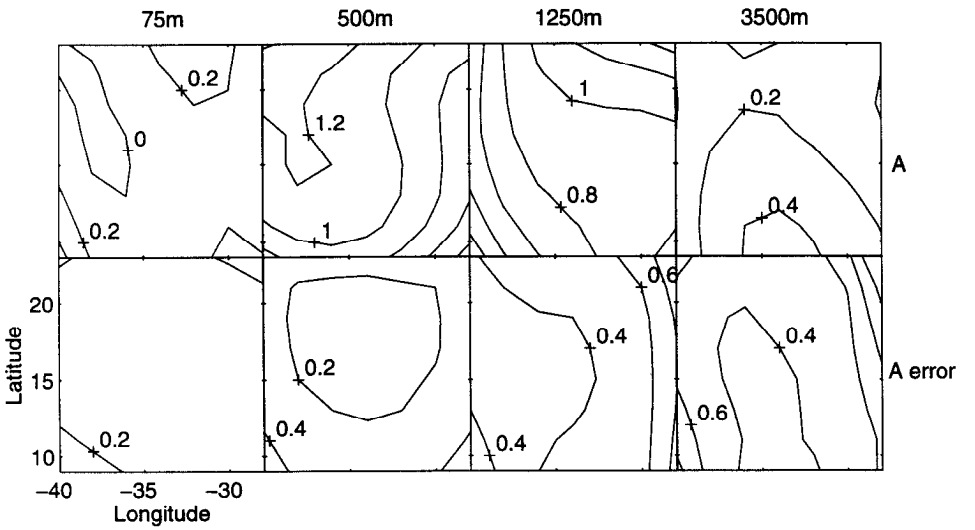

Figure 17. Estimated horizontal diffusion coefficients at four depths (upper panel) and their errors (lower panel) from the first run of the parameterization experiment in which A, K, w and the air-sea fluxes are all treated as third order polynomials. Units are 10^7 cm^2/s.

real ocean. For an overdetermined system with full rank, on the other hand, the solutions are usually obtained by minimizing the residual norm of the equations, and thus the solutions are not sensitive to the *a priori* knowledge of the true parameter values although there remain subjective factors in overdetermined systems, such as row scaling of the equations. Our knowledge of the diffusion coefficients is limited, and a spatially smoothed version of them is acceptable. These coefficients are parameterized as polynomial functions in space (e.g., Hogg, 1987; Tziperman, 1988). In this section, we examine how different parameterizations for various variables will affect the IM solutions. The following experiments are based on the standard run defined in Section 3b(iv).

A, K, w and air-sea fluxes as third order polynomials: In the first experiment, variables A, K, w and air-sea fluxes are all parameterized as third-order discrete Tchebychev polynomial functions in the horizontal plane whose coefficients vary with depth. The equation system consists of 2319 equations for 1010 unknowns and is overdetermined and of full rank. The estimated horizontal circulations are similar to those in the standard run but not as close to the GCM ocean circulations. Significant differences are found at the surface layer (25 m) and at depths greater than 1250 m. Parameterized as polynomial functions the solutions for w have smoother horizontal structures than those in the standard run and in the GCM ocean. Estimates for diffusivity A and K are no longer constant but vary horizontally and vertically (e.g. Fig. 17 for A). At mid depths, the IM estimates are not too far from the GCM ocean values—the area averages of A are of order 1×10^7 cm^2/s. At 25 m depth, the estimates for A are larger ($\sim 4 \times 10^7$ cm^2/s) than the GCM ocean value, but the differences are insignificant because of the even larger solution errors. On the other hand, at the depths

of 75, 1750, 2500, and 3500 m, the solutions for A are significantly smaller than the GCM ocean value although they are of the same order. Biased estimates for the diffusion coefficients and the velocities result in biased estimates for the air-sea heat and freshwater fluxes, which significantly differ from those in the GCM ocean although they are of the same order.

A, K and air-sea fluxes as third order polynomials while w is a pointwise unknown: The parameterization scheme used above results in some unrealistic features in the air-sea heat and freshwater fluxes (not shown) as well as in the diffusivity. If the small values of A estimated on the deepest three levels can be attributed to the large error in the heat and salt conservation equations (as in Section 3b(iii)), it is difficult to explain the small values at 75 m. In the above experiment, vertical velocity was parameterized in the same way as the diffusive variables. This treatment originated from the Zhang and Hogg (1992) scheme which used potential density coordinates on which diapycnal velocity is caused solely by diffusion processes. However, in the geopotential (z) coordinate system, vertical advection will occur with or without diffusion processes. As w is linked to the divergence of horizontal velocity via the continuity equation, small variations in u and v can change the w values significantly, and w distributions may scatter in space even if the distributions of u and v are relatively smooth. As a result, small scale structures in w should be included in the parameterization. In the following experiment, w is taken as a pointwise unknown, while the diffusivities A, K and air-sea heat and freshwater fluxes are still parameterized as the third order discrete Tchebychev polynomials. Although there now are more unknowns (1424 unknowns in 2319 equations), the equation system is still overdetermined and of full rank.

The estimated velocities are improved toward those in the GCM ocean and have smaller solution errors. The diffusion coefficients (Fig. 18) still have varying spatial structures but the deviations from the GCM ocean values are smaller. The area averages of A are around 1×10^7 cm^2/s on seven (above 1500 m) of the ten vertical levels. As in the previous case, the estimates for A are smaller than the GCM ocean value on the deepest three levels and the biases are caused by the large errors in the steady IM tracer conservation equations. The small values of A at 75 m have disappeared and the estimates for K are closer to the GCM value (of 1 cm^2/s) on all the vertical levels. Furthermore, as the estimates for velocities and diffusion coefficients are closer to their "true" values, the estimates for air-sea heat and freshwater fluxes are significantly improved although not as good as in the standard run.

4. Summary and conclusions

Inverse modeling, aimed at revealing the oceanic general circulation and mixing rates from hydrographic data, has recently intensified because of rapidly increasing amounts of observational data and advances in computer power. Comparison of inverse model results with direct measurements in the real ocean is difficult due to the lack of information. Bigg's (1985) and Killworth's and Bigg's (1988) works on testing several inverse models in two GCM oceans cast serious doubts on the reliability of inverse models, especially those

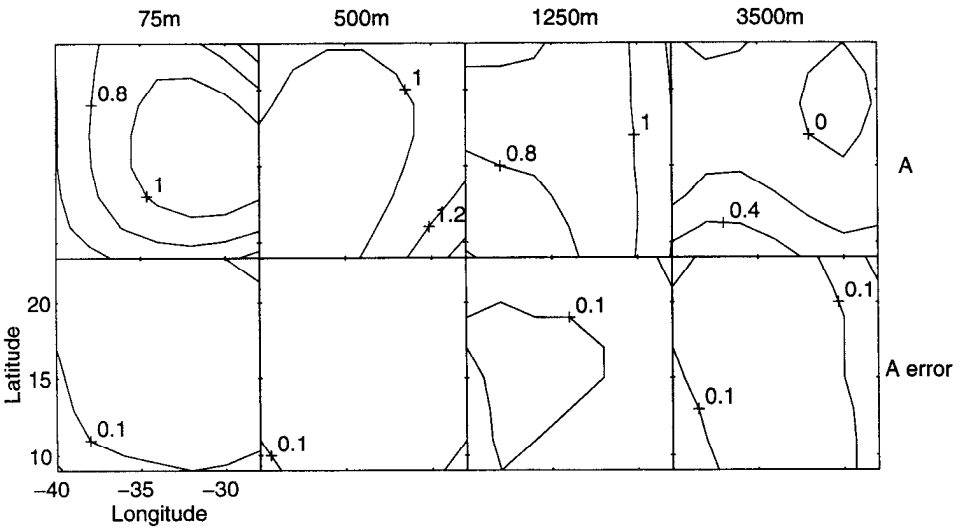

Figure 18. Same as Figure 17 but from the second run of the parameterization experiment where w is a pointwise unknown. Units are 10^7 cm^2/s.

derived from the β-spiral method. The feasibility of extracting the ocean general circulation, mixing rates, and air-sea heat and freshwater fluxes from hydrographic data by an inverse model (IM) has been pursued in the present work. The IM investigated, like the β-spiral method, is of finite difference type and assumes that the ocean general circulation is in *approximate* thermal wind balance and mass, heat, and salt are *approximately* conserved in steady state. The IM is examined in the context of a numerical model where both the physics and parameter values are known.

In this, the first of a two-paper set, the IM is applied to a non-eddy-resolving GCM ocean and we begin with application to the upper water column where the IM has higher accuracy. Although there is a rapid drop in the singular value profile of the equation system (which usually indicates possible singularity), detailed analyses show that the equation system is overdetermined and of full rank. The estimated diffusion coefficients, $A = (1.08 \pm .02) \times 10^7$ cm^2/s and $K = (1.03 \pm .01)$ cm^2/s (where errors are based on the 95% confidence interval), are close to their "true" values of unity yet the small discrepancies are significantly beyond the 95% confidence limits. The solutions for w have the same structure as the horizontally smoothed GCM ocean ones, and the estimated horizontal circulations are statistically consistent with the GCM ocean almost everywhere on all the levels but the deepest one at 1250 m where the flows are very weak although of similar pattern. These small yet significant discrepancies are caused by the different physics of the IM and the GCM ocean. In particular, the time variations in the GCM conservation equations, which are ignored in the IM, are not well represented as "white noise." Systematic offsets can lead to biased estimates.

Model errors are more important in the deep layers (e.g., larger than the diffusion terms) than in the upper ones. When we ran the IM in a deep water column, the estimates for

diffusivity, $A = (.98 \pm .01) \times 10^7$ cm^2/s and $K = .86 \pm 0.02$ cm^2/s, were further away from the GCM values. When A is allowed to be a function of depth the solutions for A are consistent with the GCM value at levels where the model errors are smaller than the diffusion terms but significant differences appear in the contrary regime. Treating the time variations as known inhomogeneous terms for the IM conservation equations instead of model errors, the IM estimates for all the parameters are consistent with the GCM values [e.g., $A = (1.03 \pm 0.05) \times 10^7$ cm^2/s, $K = (0.99 \pm 0.02)$ cm^2/s], despite the approximations used in the other equations (e.g., approximate thermal wind relation).

Present knowledge of global air-sea heat and freshwater fluxes is still poor, and an effort is made to infer these parameter values by the IM. By including the Ekman transport in the surface layer, the IM estimated air-sea fluxes not only have the same spatial patterns as those of the GCM ocean, but they are also numerically consistent within the expected errors, as is the estimated surface layer circulation. The uncertainties, however, are larger in the surface layer than in the deeper ones as more assumptions are used in the surface layer.

Experiments on different parameterizations of various variables are carried out. Parameterizing vertical velocity, diffusion coefficients and air-sea fluxes all as polynomial functions results in unreasonable estimates for some variables (e.g., the air-sea fluxes). Unlike the potential density coordinate frame, where diapycnal advection must be caused by diffusion processes, vertical velocity in geopotential z coordinates can exist without diffusion. w is linked to the divergence of horizontal velocity, and small-scale structures may appear in w even if the horizontal circulation is relatively smooth (Figs. 6 and 5). When w is taken as a pointwise unknown while the air-sea fluxes and diffusion coefficients are parameterized as polynomial functions, the IM results in plausible estimates for the variables. Overall, solutions for velocities are relatively robust, while those for diffusive variables are sensitive to the specific parameterization.

In summary, the IM is quite capable of recovering the ocean circulation and diffusion coefficients as well as air-sea heat and freshwater fluxes from the hydrographic data and the climatological wind stress. These conclusions are quite different from those of Bigg's (1985) test of the β-spiral method. One possible explanation for the discrepancy is that the IM used in this work is formulated in a more accurate way than the β-spiral method. For example, there are more constraints (heat and salt conservation) on the unknowns in this work. These constraints provide more information to reduce the uncertainties of the parameters. Exact thermal wind balance is required in the β-spiral method but not in the present work, as residuals are allowed in the conservation constraints as well as in the dynamic ones. The small deviations from the thermal wind relation may not be important for the strong upper ocean circulations, but they are important in resolving the weak deep ocean circulations, and thus the diffusive parameters as well.

Acknowledgments. We wish to thank Carl Wunsch, W. Brechner Owens, Jochem Marotzke and Michael Spall for their discussions and comments during this work. We are also grateful to Mike Spall for providing the GCM ocean data. Careful reading by three anonymous reviewers is most appreciated and helped us greatly to improve and clarify the presentation. Parts of the computation

were done on Cray computers at the National Center for Atmospheric Research and the Massachusetts Institute of Technology. This research was supported by the National Science Foundation under grant OCE-90-04396. During part of this writing HZ was supported by a fellowship from the Joint Institute for Marine Observations of Scripps Institution of Oceanography and the National Oceanic and Atmospheric Administration. This is contribution number 9067 from the Woods Hole Oceanographic Institution.

REFERENCES

Arakawa, A. and V. R. Lamb. 1977. Computational design of the basic dynamical processes of the UCLA general circulation model. Methods in Comput. Phys., *17,* Academic Press, 174–265.

Baumgartner, A. and E. Reichel. 1975. The World Water Balance. Elsevier, Amsterdam, 179 pp.

Bigg, G. R. 1985. The beta-spiral method. Deep-Sea Res., *32,* 465–484.

Bryan, K. 1969. A numerical method for the study of the circulation of the world ocean. J. Comput. Phys., *4,* 347–376.

Bryan, K. and M. D. Cox. 1972. An approximate equation of state for numerical models of ocean circulation. J. Phys. Oceanogr., *2,* 510–514.

Bryden, H. L., J. Candela and T. H. Kinder. 1994. Exchange through the Strait of Gibraltar. Prog. Oceanogr., *33,* 201–248.

Cox, M. D. 1984. A primitive equation, 3-dimensional model of the ocean. GFDL Ocean Group Tech. Rep. No. 1, 143 pp.

Fiadeiro, M. E. and G. Veronis. 1984. Obtaining velocities from tracer distributions. J. Phys. Oceanogr., *14,* 1734–1746.

Figueroa, H. A. and D. B. Olson. 1989. Lagrangian statistics in the South Atlantic as derived from SOS and FGGE drifters. J. Mar. Res., *47,* 525–546.

Han, Y. J. 1984. A numerical world ocean general circulation model. Part II: A baroclinic experiment. Dyn. Atmos. Oceans, *8,* 141–172.

Hellerman, S. and M. Rosenstein. 1983. Normal monthly wind stress over the world ocean with error estimates. J. Phys. Oceanogr., *13,* 1093–1104.

Hogg, N. 1987. A least-squares fit of the advective-diffusive equations to Levitus Atlas data. J. Mar. Res., *45,* 347–375.

Jenkins, W. J. 1987. ^{3}H and ^{3}He in the beta triangle: observations of gyre ventilation and oxygen utilization rates. J. Phys. Oceanogr., *17,* 763–783.

Killworth, P. D. and G. R. Bigg. 1988. An intercomparison of inverse methods using an eddy-resolving general circulation model. J. Phys. Oceanogr., *18,* 987–1008.

Lawson, C. L. and R. J. Hanson. 1974. Solving Least Squares Problems. Prentice-Hall, Inc., Englewood Cliffs, NJ, 340 pp.

Lee, J. H. and G. Veronis. 1989. Determining velocities and mixing coefficients from tracers. J. Phys. Oceanogr., *19,* 487–500.

—— 1993. Inversions of data from the thermohaline staircase in the western tropical North Atlantic. Deep-Sea Res. I, *40,* 1839–1862.

Levitus, S. 1982. Climatological Atlas of the World Ocean. NOAA Professional Paper 13, National Oceanic and Atmospheric Administration, Rockville, Maryland, 173 pp.

Montgomery, R. B. 1938. Circulation in upper layers of southern North Atlantic deduced with use of isentropic analysis. Pap. in Phys. Oceanogr. Meteorol., *6,* 255 pp.

Olbers, D. J., M. Wenzel and J. Willebrand. 1985. The inference of North Atlantic circulation patterns from climatological hydrographic data. Rev. Geophys., *23,* 313–356.

Pedlosky, J. 1987. Geophysical Fluid Dynamics. 2nd ed., Springer-Verlag, New York, 710 pp.

Schlitzer, R. 1987. Renewal rates of East Atlantic deep water estimate by inversion of ^{14}C data. J. Geophys. Res., *92,* 2953–2969.

Schott, F. and H. Stommel. 1978. Beta-spirals and absolute velocities in different oceans. Deep-Sea Res., *25,* 961–1010.

Spall, M. A. 1992. Cooling spirals and recirculations in the subtropical gyre. J. Phys. Oceanogr., *22,* 564–571.

Spall, M. A., P. L. Richardson and J. Price. 1993. Advection and eddy mixing in the Mediterranean salt tongue. J. Mar. Res., *51,* 797–818.

Spitzer, W. S. and W. J. Jenkins. 1989. Rates of vertical mixing, gas exchange and new production: Estimates from seasonal gas cycles in the upper ocean near Bermuda. J. Mar. Res., *47,* 169–196.

Stommel, H. and F. Schott. 1977. The beta spiral and the determination of the absolute velocity field from hydrographic station data. Deep-Sea Res., *24,* 325–329.

Tziperman, E. 1988. Calculating the time-mean oceanic general circulation and mixing coefficients from hydrographic data. J. Phys. Oceanogr., *18,* 519–525.

Wunsch, C. 1977. Determining the general circulation of the ocean: A preliminary discussion. Science, *196,* 871–875.

—— 1978. The general circulation of the North Atlantic west of 50°W determined from inverse methods. Rev. of Geophys. Space Phys., *16,* 583–620.

—— 1984. An eclectic Atlantic Ocean circulation model. Part 1: The meridional flux of heat. J. Phys. Oceanogr., *14,* 1712–1733.

—— 1988a. Eclectic modeling of the North Atlantic, Part 2: Transient tracers and the ventilation of the eastern basin thermocline. Phil. Trans. Royal Soc., *A325,* 201–236.

—— 1988b. Transient tracers as a problem in control theory. J. Geophys. Res., *93,* 8099–8110.

—— 1989. Tracer inverse problems, *in* Oceanic Circulation Models: Combining Data and Dynamics, D. L. Anderson and J. Willebrand, eds., NATO ASI Series C: Mathematical and Physical Sciences, *284,* 1–14.

Wunsch, C. and B. Grant. 1982. Towards the general circulation of the North Atlantic Ocean. Prog. Oceanogr., *11,* 1–59.

Wüst, G. 1935. Schichtung und Zirkulation des Atlantischen Ozeans. Die Stratosphäre, *in* Wissenschaftliche Ergebnisse der Deutschen Atlantischen Expedition auf dem Forschungs- und Vermessungsschiff "Meteor" 1925–1927, *6:* 1st Part, 2, 180 pp.

Zhang, H.-M. 1994. Application of an inverse model in the community modeling effort results. Ph.D. dissertation, MIT/WHOI Joint Program, 262 pp.

Zhang, H.-M. and N. G. Hogg. 1992. Circulation and water mass balance in the Brazil Basin. J. Mar. Res., *50,* 385–420.

Received: 8 August, 1995; revised: 19 March, 1996.